UCID- 17978

Lawrence Livermore Laboratory

THE NON-EQUILIBRIUM MARSHAK WAVE PROBLEM

G. C. Pomraning

August 7, 1978

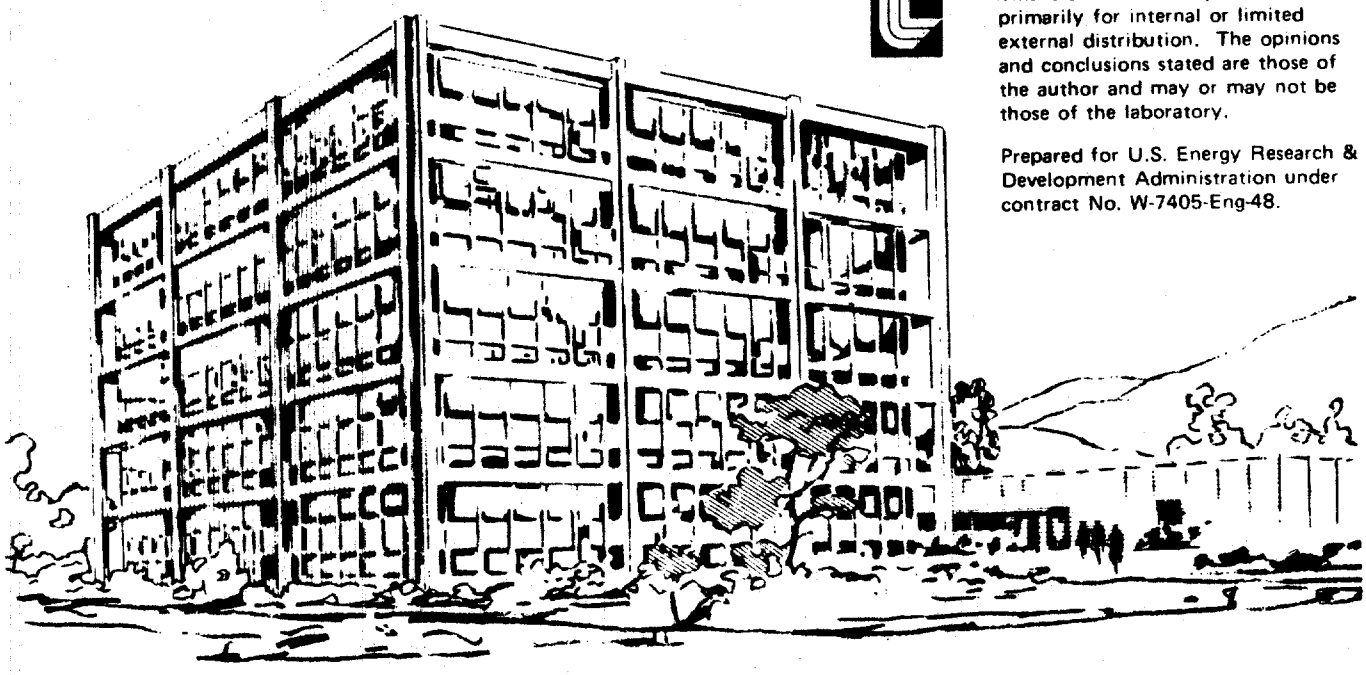

Prepared for U.S. Energy Research & Development Administration under contract No. W-7405-Eng-48.

ABSTRACT

An analytic solution to a particular Marshak problem is given. The radiative transfer model used is the gray, non-equilibrium diffusion approximation which allows the radiation and material fields to be out of equilibrium. This solution should be useful as a reference problem for validating time dependent radiative transfer computer codes, as well as investigating the convergence, as a function of space and time step size, for such codes. The coupling of the radiation field to the material field in a multigroup code, a difficult numerical problem, can also be tested against this solution. Typical numerical results are given for surface quantities, integral quantities, and the distribution of radiative energy and material temperature as a function of space and time.

"Work performed under the auspices of the U.S. Department of Energy by the Lawrence Livermore Laboratory under contract number W-7405-ENG-48."

1. Introduction

A difficult class of engineering problems is time dependent radiative transfer in which the radiation and material energy fields are allowed to interact. The difficulty stems from the underlying complexity of the equation of radiative transfer, the need to include the energy balance equation for the material in the problem description, and the generally complex dependence of the material properties (opacities and heat capacity) on the relevant independent variables.

Because of this complexity, most, if not all, realistic problems of this type must be solved numerically. Many computer codes exist in the engineering and scientific community for such problems, including the effects of hydrodynamic motion if this is an important effect. As with all computer codes, it is desirable (essential) to have benchmark or reference problems for which analytic solutions are known for purposes of verifying the numerical procedures used. In addition, such analytic solutions allow one to test the sensitivity of the code to changes in mesh size (in space or time) in an unambiguous way. Such test problems are almost nonexistent for this class of radiative transfer problems, again because of the complexity of the underlying equations.

One semi-analytic solution that does exist in the literature is the so-called Marshak wave problem[1]. In the heat transfer context, this corresponds to an initially cold halfspace of material with radiation incident upon the surface. Under the simplifications introduced by Marshak, this problem admits a similarity solution which reduces the problem to the solution of a second order nonlinear ordinary differential equation. This equation cannot be solved analytically, but numerical results have been obtained by Kass and O'Keeffe[2] in the context of chemical diffusion.

The solution exhibits a wavefront which penetrates the slab with the characteristic square root of time behavior. To obtain this semi-analytical solution, Marshak made the assumption that the material and radiation fields are in equilibrium; i.e., the radiation field at any space and time point is Planckian at the local material temperature. This has the great simplifying effect of eliminating the equation of transfer from the problem. Modern radiative transfer treatments do not in general make this simplifying assumption. The radiation and material fields are allowed to develop separately according to a more accurate physical description, with an interaction term between the two fields which allows equilibration only when the physics of the problem dictates such an equilibrium.

In this paper, we give a solution to the Marshak wave problem allowing non-equilibrium between the radiation and material fields. In order to make the problem tractable analytically, we need introduce a specific dependence of the material heat capacity on the material temperature. We assume that this heat capacity is proportional to the cube of the temperature. Because of this, our solution probably does not correspond to any interesting physical problem, as does the classic Marshak treatment. However, our intent is different from that of Marshak. He was interested in modeling, in a semi-quantitative manner, a particular physical phenomena. This necessitated simplifying the equations to the point where a solution was possible, while maintaining as much as possible the essential physics of the problem. We wish to maintain the underlying equations and are willing to relax the physical content of the problem to obtain a detailed solution. Radiative transfer codes are meant to handle an arbitrary temperature dependence of the heat capacity, and thus the

solution presented here should provide a useful test problem for such codes.

To our knowledge, no other analytic solution, allowing for non-equilibrium in a time dependent problem, exists in the literature. We regard the present solution as a first step in generating useful test problems. Hopefully, other solutions, involving more detailed physics, can be generated in the future to give additional test problems against which radiative transfer codes can be validated.

2. The Problem and General Solution

We consider a semi-infinite purely absorbing medium occupying $0 \leq z < \infty$. The medium is assumed to be homogeneous and, at t=0, to be at a zero temperature with no radiation field present. Commencing at t=0, we allow a time independent radiative flux to impinge upon the face at z=0. We wish to compute, as a function of space and time, the material temperature and the radiation field. Hydrodynamic motion and heat conduction are assumed unimportant, and the radiative transfer is modeled as a one group (gray) process in the diffusion (P-1 or two T) description. The equation of transfer is then[3]

$$\frac{\partial E_r(z,t)}{\partial t} - \frac{\partial}{\partial z}\left[\frac{c}{3\kappa(T)}\frac{\partial E_r(z,t)}{\partial z}\right] = c\kappa(T)\left[aT^4(z,t)-E_r(z,t)\right] , \qquad (1)$$

where z is the spatial variable, t is the temporal variable, $E_r(z,t)$ is the radiation energy density, $T(z,t)$ is the material temperature, $\kappa(T)$ is the absorption cross section (opacity), c is the speed of light, and a is the radiation constant. The Marshak (Milne) boundary condition on Eq. (1) at z=0 is

$$E_r(0,t) - \left(\frac{2}{3\kappa[T(0,t)]}\right)\frac{\partial E_r(0,t)}{\partial z} = \frac{4}{c}F_{inc} , \qquad (2)$$

where F_{inc} is the flux incident upon the medium at z=0. At $z=\infty$, we have the boundary condition

$$E_r(\infty,t) = 0 . \qquad (3)$$

The initial condition is that of no radiation present, i.e.,

$$E_r(z,0) = 0 . \qquad (4)$$

The material energy balance equation is

$$c_v(T)\frac{\partial T(z,t)}{\partial t} = c\kappa(T)\left[E_r(z,t) - aT^4(z,t)\right] , \qquad (5)$$

where $c_v(T)$, the heat capacity per unit volume, is related to the material energy density E_m by

$$E_m(T) = \int_0^T dT' c_v(T') \ . \tag{6}$$

The initial condition on Eq. (5) is taken to be

$$T(z,0) = 0 \ . \tag{7}$$

Equations (1) and (5), together with the boundary and initial conditions, Eqs. (2), (3), (4), and (7), constitute two equations for the two unknowns $E_r(z,t)$ and $T(z,t)$. For a general temperature dependence of $\kappa(T)$ and $c_v(T)$, these equations are clearly nonlinear. However, if we consider the classic radiative transfer problem of κ independent of temperature, and further assume c_v proportional to T^3, i.e.,

$$c_v = \alpha T^3 \ , \tag{8}$$

then our equations become linear in E_r and T^4, and we can use classic analysis to obtain a solution. Before proceeding with the solution, we recast the equations into dimensionless form. We write the incident flux in terms of an effective temperature θ_{inc} as.

$$F_{inc} = \sigma\theta_{inc}^4 \ , \tag{9}$$

where σ is the Stefan-Boltzmann constant, $\sigma = ac/4$. Additionally, we define a radiation temperature $\theta(z,t)$ by the equation

$$E_r(z,t) = a\theta^4(z,t) \ . \tag{10}$$

We introduce the dimensionless independent variables

$$x \equiv \sqrt{3}\kappa z \ , \tag{11}$$

$$\tau \equiv \left(\frac{16\sigma\kappa}{\alpha}\right)t \ , \tag{12}$$

and define new dependent variables as

$$u(x,\tau) \equiv \left[\frac{\theta(z,t)}{\theta_{inc}}\right]^4 , \tag{13}$$

$$v(x,\tau) \equiv \left[\frac{T(z,t)}{\theta_{inc}}\right]^4 . \tag{14}$$

Then Eqs. (1) and (5) take the dimensionless form

$$\varepsilon \frac{\partial u(x,\tau)}{\partial \tau} - \frac{\partial^2 u(x,\tau)}{\partial x^2} = v(x,\tau) - u(x,\tau) , \tag{15}$$

$$\frac{\partial v(x,\tau)}{\partial \tau} = u(x,\tau) - v(x,\tau) , \tag{16}$$

where we have defined the parameter

$$\varepsilon \equiv \frac{16\sigma}{c\alpha} . \tag{17}$$

The boundary and initial conditions, Eqs. (2), (3), (4), and (7) become in these new variables

$$u(0,\tau) - \frac{2}{\sqrt{3}} \frac{\partial u(0,\tau)}{\partial x} = 1 , \tag{18}$$

$$u(\infty,\tau) = u(x,0) = v(x,0) = 0 . \tag{19}$$

Equations (15) through (19) are the equations we shall solve.

Setting the parameter ε to zero corresponds to the "no retardation" approximation. That is, $\varepsilon=0$ is equivalent to assuming that, as far as the radiative transfer process is concerned, the speed of light is infinite. This implies that the radiation field instantly comes into a steady state distribution with the material temperature distribution at any time t. It should be emphasized that $\varepsilon=0$ does *not* imply $u=v$ ($E_r=E_m$), because Eq. (15) contains a spatial streaming term. Only in the absence of spatial gradients does the $\varepsilon=0$ approximation imply $u=v$, i.e., complete thermodynamic equilibrium.

The classic Marshak treatment corresponds to setting $\epsilon = 0$ and ignoring spatial gradients in the equation of transfer, thus obtaining $u=v$, or, equivalently, assuming the radiation field to be Planckian at the local temperature.

Before proceeding with the solution, it may be useful to say a few words about the radiative transfer model we have employed. Rather than dealing with the more complex integro-differential or integral equation of transfer, we have used the lowest order spherical harmonic approximation, commonly called the P-1 or 2-T diffusion approximation. One would expect, and experience bears it out, that for optically thick systems the P-1 approximation should be quite accurate. This is the case for the Marshak wave problem. Thus our solution is a rigorous test problem for codes using the P-1 approximation, but in addition provides a reasonably good test problem for transport codes as well. We have also used a one group, or gray, radiative transfer description. Again, for optically thick systems such a description is often adequate. However, even the multigroup aspect of multigroup codes can be partially tested against the solution given here. If the code is used in a multigroup mode to compute a problem in which the opacity is, in fact, independent of frequency, then a one group description is rigorously correct, and the present test problem gives the analytic result. This is particularly important since the coupling of the radiation field to the material is a difficult aspect of multigroup codes. This aspect can be tested, as just described, against the analytic solution given here.

To solve Eqs. (15) through (19), we introduce the Laplace transform $\bar{f}(s)$ of a function $f(\tau)$ by the definition

$$\bar{f}(s) \equiv \int_0^\infty d\tau e^{-s\tau} f(\tau) \ . \tag{20}$$

Taking the Laplace transform of Eqs. (15), (16), (18), and (19) gives

$$\varepsilon s\bar{u}(x,s) - \frac{\partial^2 \bar{u}(x,s)}{\partial x^2} = \bar{v}(x,s) - \bar{u}(x,s) \ , \tag{21}$$

$$s\bar{v}(x,s) = \bar{u}(x,s) - \bar{v}(x,s) \ , \tag{22}$$

$$\bar{u}(0,s) - \frac{2}{\sqrt{3}} \frac{\partial \bar{u}(0,s)}{\partial x} = \frac{1}{s} \ , \tag{23}$$

$$\bar{u}(\infty,s) = 0 \ . \tag{24}$$

Equation (22) gives

$$\bar{v}(x,s) = (\frac{1}{s+1})\bar{u}(x,s) \ , \tag{25}$$

and using this in Eq. (21) gives

$$\frac{\partial^2 \bar{u}(x,s)}{\partial x^2} = \beta^2(s)\bar{u}(x,s) \ , \tag{26}$$

where we have defined

$$\beta^2(s) \equiv (\frac{s}{s+1})[1+\varepsilon(s+1)] \ . \tag{27}$$

The solution to Eq. (26) subject to the boundary condition at $x=\infty$, Eq. (24), is

$$\bar{u}(x,s) = K(s)e^{-\beta(s)x} \ . \tag{28}$$

The constant $K(s)$ is determined from the condition at $x=0$, Eq. (23). We find

$$\bar{u}(x,s) = \frac{\sqrt{3}e^{-\beta(s)x}}{s[\sqrt{3}+2\beta(s)]} \ , \tag{29}$$

and Eq. (25) then gives

$$\bar{v}(x,s) = \frac{\sqrt{3}e^{-\beta(s)x}}{s(s+1)[\sqrt{3}+2\beta(s)]} . \tag{30}$$

The solutions for $u(x,\tau)$ and $v(x,\tau)$ follow from Eqs. (29) and (30) by the Laplace inversion theorem

$$f(\tau) = \frac{1}{2\pi i}\int_C ds e^{s\tau}\bar{f}(s) , \tag{31}$$

where the integration contour C is a line parallel to the imaginary s axis to the right of all the singularities of $\bar{f}(s)$.

From the large s and small s limits of Eqs. (29) and (30), relating thse to the small τ and large τ limits of $u(x,\tau)$ and $v(x,\tau)$, respectively, we have

$$u(x,0) = v(x,0) = 0 , \tag{32}$$

$$u(x,\tau) \underset{\tau\to\infty}{\to} v(x,\tau) \underset{\tau\to\infty}{\to} 1 , \tag{33}$$

where we have used the theorems

$$\lim_{s\to\infty}[s\bar{f}(s)] = \lim_{\tau\to 0}[f(\tau)] , \tag{34}$$

$$\lim_{s\to 0}[s\bar{f}(s)] = \lim_{\tau\to\infty}[f(\tau)] . \tag{35}$$

Equation (32) is just a restatement of the initial condition [see Eq. (19)], and Eq. (33) states that at infinite time, both the radiation and material temperatures approach a constant, equal to the temperature of the impinging flux.

3. The Solution for $\varepsilon=0$

Because of the complex s dependence of $\bar{u}(x,s)$ and $\bar{v}(x,s)$ as given by Eqs. (27), (29), and (30), we initially consider the $\varepsilon=0$, no retardation, case. We reexamine, for $\varepsilon=0$, the limits at $\tau=0$ and $\tau=\infty$. We find, at $\tau=\infty$,

$$u(x,\tau) \underset{\tau\to\infty}{\to} v(x,\tau) \underset{\tau\to\infty}{\to} 1 \ , \tag{36}$$

just as before. However, for $\tau=0$ we find a different behavior since $\beta(s)$ behaves differently as $s\to\infty$ for $\varepsilon=0$, i.e., $\beta(\infty) = 1$ for $\varepsilon=0$. This gives

$$u(x,0) = \frac{\sqrt{3}e^{-x}}{(\sqrt{3}+2)} \ , \tag{37}$$

$$v(x,0) = 0 \ . \tag{38}$$

That is, the material field is still zero at $\tau=0$, consistent with the initial condition, but the radiation field is not zero at $\tau=0$ for $\varepsilon=0$. This is because the radiation field, in the absence of retardation effects, immediately comes to a steady state consistent with a zero material field, but corresponding to an incoming flux of radiation. Equation (37) is just the steady state solution of the P-1 approximation under these conditions. Thus for a small, but non zero value of ε, the solution for $u(x,\tau)$ will exhibit a boundary layer in the time variable, leading to a rapidly varying time behavior for small times.

If we examine the surface behavior of the radiation and material fields as a function of time, we need invert, using

$$\beta(s) = \left[\frac{s}{s+1}\right]^{\frac{1}{2}} \tag{39}$$

in Eqs. (29) and (30) at x=0,

$$\bar{u}(0,s) = \frac{\sqrt{3}\ \sqrt{s+1}}{s[\sqrt{3}\ \sqrt{s+1} + 2\sqrt{s}]} \ , \tag{40}$$

$$\bar{v}(0,s) = \frac{\sqrt{3}\,\sqrt{s+1}}{s(s+1)\left[\sqrt{3}\,\sqrt{s+1} + 2\sqrt{s}\right]} \,. \tag{41}$$

The singularities of $\bar{u}(0,s)$ and $\bar{v}(0,s)$ are clearly identical, and include branch points at s=0 and s=-1. We define the proper branches as those which give a positive square root for s lying on the real positive axis. Extending both branch cuts along the negative real axis, we have a composite branch cut for $-1 \leq s \leq 0$. The functions are analytic on the negative real axis for $s < -1$, the effects of the two branch cuts having cancelled. These functions also have a simple pole at s=0. A second pole exists at s=3, but this pole lies on the non physical Riemann sheet and need not be considered. The Laplace inversion integral for either $\bar{u}(0,s)$ or $\bar{v}(0,s)$ is then a straight vertical line in the right half s plane. Closing this contour in the left half plane, one finds, as usual, that the large semicircle gives a zero contribution, with contributions coming from the branch cut and the pole at s=0. Defining a new integration variable $\xi=-s$, we find, omitting the algebraic detail,

$$u(0,\tau) = 1 - \frac{2\sqrt{3}}{\pi}\int_0^1 d\xi\left(\frac{1-\xi}{\xi}\right)^{\frac{1}{2}}\left(\frac{1}{3+\xi}\right)e^{-\xi\tau} \,, \tag{42}$$

$$v(0,\tau) = 1 - \frac{2\sqrt{3}}{\pi}\int_0^1 d\xi\left[\xi(1-\xi)\right]^{-\frac{1}{2}}\left(\frac{1}{3+\xi}\right)e^{-\xi\tau} \,. \tag{43}$$

These integrals must be performed numerically. To remove the integrable singularity at $\xi=0$ in Eq. (42), we change integration variables according to $\xi=\eta^2$, and find

$$u(0,\tau) = 1 - \frac{4\sqrt{3}}{\pi}\int_0^1 d\eta\,\frac{(1-\eta^2)^{\frac{1}{2}}}{(3+\eta^2)}\,e^{-\tau\eta^2} \,, \tag{44}$$

a form suitable for numerical integration. Equation (43) has integrable singularities at both $\xi=0$ and $\xi=1$. To remove these, we note

$$[\xi(1-\xi)]^{-\frac{1}{2}} = [(1-\xi)/\xi]^{\frac{1}{2}} + [\xi/(1-\xi)]^{\frac{1}{2}} , \tag{45}$$

and change integration variables according to $\xi=\eta^2$ in the first term and $1-\xi=\eta^2$ in the second. This gives

$$v(0,\tau) = 1 - \frac{4\sqrt{3}}{\pi}\int_0^1 d\eta\, \frac{(1-\eta^2)^{\frac{1}{2}}}{(3+\eta^2)} e^{-\tau\eta^2} - \frac{4\sqrt{3}}{\pi}\int_0^1 d\eta\, \frac{(1-\eta^2)^{\frac{1}{2}}}{(4-\eta^2)} e^{-\tau(1-\eta^2)} . \tag{46}$$

or,

$$v(0,\tau) = u(0,\tau) - \frac{4\sqrt{3}}{\pi}\int_0^1 d\eta\, \frac{(1-\eta^2)^{\frac{1}{2}}}{(4-\eta^2)} e^{-\tau(1-\eta^2)} , \tag{47}$$

which shows, as expected on physical grounds, that the material field always lags behind the radiation field. Both Eqs. (44) and (46) can be integrated analytically for $\tau=0$, and one finds results consistent with Eqs. (37) and (38), providing a partial check on these integral expressions.

The flux of radiation is given by

$$F(z,t) = -\frac{c}{3\kappa}\frac{\partial E_r(z,t)}{\partial z} , \tag{48}$$

or, if we introduce the dimensionless variables x and τ, and define

$$w(x,\tau) \equiv \frac{F(z,t)}{F_{inc}} , \tag{49}$$

we have

$$w(x,\tau) = -\frac{4}{\sqrt{3}}\frac{\partial u(x,\tau)}{\partial x} . \tag{50}$$

Laplace transforming this result, and using Eq. (29) for $\bar{u}(x,s)$, we find for $\varepsilon=0$ that the Laplace transform of the surface flux is given by

$$\bar{w}(0,s) = \frac{4}{\sqrt{3s(s+1)} + 2s} . \tag{51}$$

By examining the small and large s behavior of Eq. (15), we find

$$w(0,\tau) \underset{\tau\to\infty}{\to} 0 \ , \tag{52}$$

$$w(0,0) = \frac{4}{\sqrt{3}+2} \ . \tag{53}$$

The infinite time limit is just a manifestation that at infinite time the entire halfspace is at a constant temperature with a uniform radiation field [see Eq. (33)] and hence there is no gradient and no flux. At $\tau=0$, physically one should find that all of the impinging radiation is absorbed, with no reradiation because the material is cold. That is, we should have $w(0,0) = 1$, whereas Eq. (53) states

$$w(0,0) = 1.0718 \tag{54}$$

This 7% error is associated with the Marshak boundary condition applied to the P-1 approximation, Eq. (2), as has been discussed in detail recently[4].

For a general value of τ, we invert Eq. (51) in a manner similar to our previous inversions of $\bar{u}(0,\tau)$ and $\bar{v}(0,\tau)$. In this case, however, there is no pole at s=0. We find

$$w(0,\tau) = \frac{8\sqrt{3}}{\pi}\int_0^1 d\eta \ \frac{(1-\eta^2)^{\frac{1}{2}}}{(3+\eta^2)} \ e^{-\tau\eta^2} \ . \tag{55}$$

We note the similarity of this result to that for $u(0,\tau)$ as given by Eq. (44). Combining these two results, we have

$$u(0,\tau) + \frac{1}{2}\, w(0,\tau) = 1 \ , \tag{56}$$

which is just a restatement of the Marshak boundary condition, Eq. (18), as can be seen by using the definition of $w(x,\tau)$, Eq. (50), in Eq. (56).

Of perhaps more interest than these surface quantities are the integrated radiation and material energies in the slab as a function of time. We define these integral quantities as

$$\mathscr{E}_r(\tau) \equiv \int_0^\infty dz E_r(z,t) = \left(\frac{a\theta_{inc}^4}{\sqrt{3}\kappa}\right)\int_0^\infty dx u(x,\tau) \ , \tag{57}$$

and

$$\mathscr{E}_m(\tau) \equiv \frac{\alpha}{4}\int_0^\infty dz T^4(z,t) = \left(\frac{\alpha\theta_{inc}^4}{4\sqrt{3}\kappa}\right)\int_0^\infty dx v(x,\tau) \ . \tag{58}$$

We define dimensionless integral energies $\psi_r(\tau)$ and $\psi_m(\tau)$ as

$$\psi_r(\tau) \equiv \frac{\mathscr{E}_r(\tau)}{\mathscr{E}_r^{(0)}} \ , \tag{59}$$

$$\psi_m(\tau) \equiv \frac{\mathscr{E}_m(\tau)}{\mathscr{E}_m^{(0)}} \ , \tag{60}$$

where

$$\mathscr{E}_r^{(0)} \equiv \frac{a\theta_{inc}^4}{\sqrt{3}\kappa} \ , \tag{61}$$

$$\mathscr{E}_m^{(0)} \equiv \frac{\alpha\theta_{inc}^4}{4\sqrt{3}\kappa} \ . \tag{62}$$

Physically, $\mathscr{E}_r^{(0)}$ is the radiation energy in a slab of thickness one diffusion length $(\sqrt{3}\kappa)^{-1}$ with a uniform radiation temperature θ_{inc}. Likewise, $\mathscr{E}_m^{(0)}$ is the material energy in a slab of thickness one diffusion length with a uniform material temperature θ_{inc}. Combining Eqs. (57) through (62) we have

$$\psi_r(\tau) = \int_0^\infty dx u(x,\tau) \ , \tag{63}$$

$$\psi_m(\tau) = \int_0^\infty dx v(x,\tau) \ . \tag{64}$$

To compute these integrals, we Laplace transform Eqs. (63) and (64), use Eqs. (29) and (30) for $\bar{u}(x,s)$ and $\bar{v}(x,s)$, setting $\epsilon=0$, and perform the indicated integrals over x. We find

$$\bar{\psi}_r(s) = \frac{\sqrt{3}(s+1)}{s(\sqrt{3s(s+1)} + 2s)} , \tag{65}$$

and

$$\bar{\psi}_m(s) = \frac{\sqrt{3}}{s(\sqrt{3s(s+1)}+2s)} . \tag{66}$$

Examining the large s (small τ) limit of these expressions, we find

$$\psi_r(0) = \frac{\sqrt{3}}{\sqrt{3}+2} , \tag{67}$$

$$\psi_m(0) = 0 , \tag{68}$$

which are correct [see Eqs. (37) and (38)]. For small s we find

$$\bar{\psi}_r(s) \underset{s\to 0}{\to} \bar{\psi}_m(s) \underset{s\to 0}{\to} s^{-3/2} \tag{69}$$

and hence we have

$$\psi_r(\tau) \underset{\tau\to\infty}{\to} \psi_m(\tau) \underset{\tau\to\infty}{\to} 2\sqrt{\tau/\pi} , \tag{70}$$

the familiar $\sqrt{\tau}$ dependence.

To obtain the results for a general τ, we once again close the inversion contours in the left half plane, wrapping around the branch cuts covering $-1 \leq s < 0$, and integrating around a small circle centered at s=0. We note that near s=0 both $\bar{\psi}_r(s)$ and $\bar{\psi}_m(s)$ behave like $s^{-3/2}$ [see Eq. (69)], and care must be taken in evaluating the integrals near s=0. In particular, both the branch cut contributions and the small circle contribution separately diverge. Thus one must integrate the branch cut contributions from -1 to $-\delta$, integrate around a small circle of radius δ centered at s=0, analytically combine the results, and then let δ go to zero. The separate singularities in δ cancel, and the resulting combined integrals are finite. As earlier, one must then make a change of variables to put the results in a form suitable for numerical integration. Omitting the considerable algebraic

detail, we find

$$\psi_r(\tau) = \frac{2}{\pi}\int_0^1 d\eta\left[2\tau + \left(\frac{7+4\sqrt{1-\eta^2}-3\eta^2}{1+\sqrt{1-\eta^2}}\right)\left(\frac{1}{3+\eta^2}\right)\right]e^{-\tau\eta^2} + \frac{2}{\pi}e^{-\tau} - \frac{2}{\sqrt{3}}, \quad (71)$$

and

$$\psi_m(\tau) = \frac{2}{\pi}\int_0^1 d\eta\left[2\tau + \left(\frac{4+\sqrt{1-\eta^2}}{1+\sqrt{1-\eta^2}}\right)\left(\frac{1}{3+\eta^2}\right)\right]e^{-\tau\eta^2} + \frac{2}{\pi}e^{-\tau} - \frac{2}{\sqrt{3}}. \quad (72)$$

For $\tau=0$, analytic integration of Eqs. (71) and (72) reproduces Eqs. (67) and (68), and for large τ, Eqs. (71) and (72) give the proper asymptotic behavior, Eq. (70). Two additional checks on the accuracy of Eqs. (71) and (72) can be made. First, it can be shown that these two results satisfy

$$\frac{\partial\psi_m(\tau)}{\partial\tau} = \psi_r(\tau) - \psi_m(\tau), \quad (73)$$

which is just the overall energy balance equation for the material, obtained by integrating Eq. (16) over all x. Secondly, it can also be shown that these two results, together with the result for $w(0,\tau)$ given by Eq. (55), satisfy

$$-\frac{\sqrt{3}}{4}w(0,\tau) = \psi_m(\tau) - \psi_r(\tau), \quad (74)$$

which is just the integral over x of the equation of transfer, Eq. (15), with $\varepsilon=0$.

Numerical results for the three surface quantities $u(0,\tau)$, $v(0,\tau)$ and $w(0,\tau)$, given by Eqs. (44), (46), and (55), as well as the two integral quantities $\psi_r(\tau)$ and $\psi_m(\tau)$, given by Eqs. (71) and (72), are given in Table I. The values were computed by dividing the integration range $0 \le \eta \le 1$ for each integral into N equal intervals, and performing a 16 point Gauss quadrature in each interval. N was successively doubled until the desired accuracy was achieved. The values in Table I were obtained by

specifying a fractional absolute error of 10^{-5} for each integral. The values given are believed to be accurate to the number of digits given.

Finally, one can, by inverting the transforms u(x,s) and v(x,s), obtain results for the radiation energy and material temperature fields. The results are

$$u(x,\tau) = 1 - \frac{4\sqrt{3}}{\pi}\int_0^1 d\eta\left[\frac{\sqrt{1-\eta^2}}{(3+\eta^2)}\right]\cos\left(\frac{\eta x}{\sqrt{1-\eta^2}}\right)e^{-\tau\eta^2}$$

$$- \frac{6}{\pi}\int_0^1 d\eta\left[\frac{(1-\eta^2)}{(3+\eta^2)}\right]\sin\left(\frac{\eta x}{\sqrt{1-\eta^2}}\right)e^{-\tau\eta^2}, \qquad (75)$$

and

$$v(x,\tau) = 1 - \frac{4\sqrt{3}}{\pi}\int_0^1 d\eta\left[\frac{\sqrt{1-\eta^2}}{(3+\eta^2)}\right]\cos\left(\frac{\eta x}{\sqrt{1-\eta^2}}\right)e^{-\tau\eta^2}$$

$$- \frac{4\sqrt{3}}{\pi}\int_0^1 d\eta\left[\frac{\sqrt{1-\eta^2}}{(4-\eta^2)}\right]\cos\left(\frac{\sqrt{1-\eta^2}\,x}{\eta}\right)e^{-\tau(1-\eta^2)}$$

$$- \frac{6}{\pi}\int_0^1 d\eta\left[\frac{1}{\eta(3+\eta^2)}\right]\sin\left(\frac{\eta x}{\sqrt{1-\eta^2}}\right)e^{-\tau\eta^2}. \qquad (76)$$

Numerical results for representative values of x and τ are given in Table II. The same integration scheme as previously described was used to compute these integrals. However, the oscillations in the integrand due to the trigonometric functions made these integrals extremely hard to converge. A looser convergence criteria of 10^{-4} was used, and even then, for small τ, values of N as large as 16,000 were required.

4. The Solution for $\varepsilon \neq 0$

One could repeat the inversion analysis for a non-zero value of ε in a straightforward way. The algebra, however, is very much more complex. For this reason, we restricted our attention for $\varepsilon \neq 0$ to the integral quantities $\psi_r(\tau)$ and $\psi_m(\tau)$. These quantities are of primary interest in most radiative transfer problems. Laplace transforming Eqs. (63) and (64), the defining equations for $\psi_r(\tau)$ and $\psi_m(\tau)$, using Eqs. (29) and (30) for $\bar{u}(x,s)$ and $\bar{v}(x,s)$, integrating over x, and using Eq. (27) for $\beta(s)$ yields

$$\bar{\psi}_r(s) = \frac{\sqrt{3}(s+1)}{s^{3/2}[1+\varepsilon(s+1)]^{1/2}\{\sqrt{3(s+1)} + 2\sqrt{s}[1+\varepsilon(s+1)]^{1/2}\}} , \tag{77}$$

and

$$\bar{\psi}_m(s) = \frac{\sqrt{3}}{s^{3/2}[1+\varepsilon(s+1)]^{1/2}\{\sqrt{3(s+1)} + 2\sqrt{s}[1+\varepsilon(s+1)]^{1/2}\}} . \tag{78}$$

Examining the large s (small τ) limit of these equations, we find

$$\psi_r(0) = \psi_m(0) = 0 , \tag{79}$$

the physically correct limits. For small s we find

$$\bar{\psi}_r(s) \underset{s\to 0}{\to} \bar{\psi}_m(s) \underset{s\to 0}{\to} \frac{1}{\sqrt{1+\varepsilon}s^{3/2}} , \tag{80}$$

and hence we have the large time behavior

$$\psi_r(\tau) \underset{\tau\to\infty}{\to} \psi_m(\tau) \underset{\tau\to\infty}{\to} 2\left[\frac{\tau}{\pi(1+\varepsilon)}\right]^{1/2} . \tag{81}$$

Again we find the expected $\sqrt{\tau}$ dependence for large times.

To invert Eqs. (77) and (78), we need identify the singularities of the integrands. These singularities are the same for each integral, and include branch points at s=0, s=-1, and s=-(1+ε)/ε. The branches to be used in the integration are again defined as those which give positive square roots for s lying on the real positive axis. Extending all three branch cuts along the negative real axis, we find cancellation of branch

cuts for $-(1+\varepsilon)/\varepsilon \leq s \leq -1$. Thus we have effective branch cuts on the intervals $-\infty < s \leq -(1+\varepsilon)/\varepsilon$ and $-1 \leq s \leq 0$. As for the $\varepsilon=0$ case, care must be taken in integrating near s=0 since the integrands vary as $s^{-3/2}$ near s=0. In addition, the integrands each have two simple poles at

$$s = -(\frac{1}{8\varepsilon})[1 + 4\varepsilon \pm \sqrt{1+56\varepsilon+16\varepsilon^2}] \ . \tag{82}$$

However, both of these poles are easily shown to be on the nonphysical Riemann sheet, and hence can be ignored.

Omitting the straightforward, but tedious, algebraic detail, the results are

$$\psi_r(\tau) = \frac{2}{\pi\sqrt{1+\varepsilon}} \int_0^1 d\eta g_r(\tau,\eta) e^{-\tau\eta^2}$$

$$- \frac{6}{\pi} e^{-\tau} \int_0^1 d\eta h_r(\eta) \exp[-\frac{\tau}{\varepsilon(1-\eta^2)}] - \frac{2}{\sqrt{3}} \ , \tag{83}$$

and

$$\psi_m(\tau) = \frac{2}{\pi\sqrt{1+\varepsilon}} \int_0^1 d\eta g_m(\tau,\eta) e^{-\tau\eta^2} + \frac{2}{\pi\sqrt{1+\varepsilon}} e^{-\tau}$$

$$+ \frac{6\varepsilon}{\pi} e^{-\tau} \int_0^1 d\eta h_m(\eta) \exp[-\frac{\tau}{\varepsilon(1-\eta^2)}] - \frac{2}{\sqrt{3}} \ , \tag{84}$$

where

$$h_r(\eta) = \frac{(1-\eta^2)^{1/2}}{[1+\varepsilon(1-\eta^2)]^{3/2}[3+(1+4\varepsilon)\eta^2-4\varepsilon\eta^4]} \ , \tag{85}$$

$$h_m(\eta) = (1-\eta^2)h_r(\eta) \ , \tag{86}$$

$$g_m(\tau,\eta) = 2\tau + \frac{1+4\varepsilon(1-\eta^2)}{3+(4\varepsilon+1)\eta^2-4\varepsilon\eta^4}$$

$$+ \frac{3}{[1+\varepsilon(1-\eta^2)]^{1/2}[3+(4\varepsilon+1)\eta^2-4\varepsilon\eta^4]\{[1+\varepsilon(1-\eta^2)]^{1/2}+[(1+\varepsilon)(1-\eta^2)]^{1/2}\}} \ , \tag{87}$$

$$g_r(\tau,\eta) = (1-\eta^2)g_m(\tau,\eta) + 2 \ . \qquad (88)$$

Numerical results were obtained from these equations with the previously described integration routine, using a fractional convergence criteria of 10^{-5}. These results are given in Tables III and IV for a few representative values of ε. We note, as expected, that the material field always lags behind the radiation field.

5. Concluding Remarks

We have presented in this paper an analytic solution to the Marshak wave problem which should be a useful reference solution for validating time dependent radiative transfer computer codes. The solution was obtained in the form of finite integrals which had to be evaluated numerically. Typical numerical results were given to an accuracy of 10^{-4} for the pointwise, in space and time, distributions of the radiative energy and material temperatures, and 10^{-5} for surface quantities and integral energy content.

It is hoped that in the future other such reference solutions can be generated. The goal should be to find solvable problems that represent the relevant physics in more detail than the solution given here. This goal may be elusive, however, due to the complexities, including complicated equations, complicated functional forms, and nonlinearities, of the underlying equations describing the time dependent radiative energy field and its interaction and energy exchange with the material field.

REFERENCES

1. R. E. Marshak, Phys. Fluids, 1, 24 (1958).

2. W. Kass and M. O'Keeffe, J. Appl. Phys., 37, 2377 (1966).

3. G. C. Pomraning, The Equations of Radiation Hydrodynamics, Chapter III, Pergamon Press, Oxford (1973).

4. G. C. Pomraning and G. M. Foglesong, "Transport-Diffusion Interfaces in Radiative Transfer", J. Comp. Phys., submitted for publication.

TABLE I

Surface and Integral Quantities for $\epsilon = 0$

τ	$u(0,\tau)$	$v(0,\tau)$	$w(0,\tau)$	$\psi_r(\tau)$	$\psi_m(\tau)$
0.01	0.46534	0.00462	1.0693	0.46767	0.00463
0.02	0.46657	0.00921	1.0669	0.47122	0.00926
0.04	0.46903	0.01829	1.0619	0.47831	0.01847
0.07	0.47266	0.03167	1.0547	0.48891	0.03222
0.1	0.47624	0.04475	1.0475	0.49947	0.04588
0.2	0.48782	0.08638	1.0244	0.53429	0.09073
0.4	0.50941	0.16120	0.98117	0.60241	0.17754
0.7	0.53833	0.25547	0.92334	0.70098	0.30116
1.0	0.56368	0.33230	0.87264	0.79561	0.41774
2.0	0.62890	0.50386	0.74220	1.0869	0.76553
4.0	0.70709	0.65960	0.58581	1.5871	1.3335
7.0	0.76802	0.74905	0.46395	2.2074	2.0065
10.	0.80238	0.79164	0.39524	2.7321	2.5610
20.	0.85732	0.85362	0.28535	4.1198	3.9962
40.	0.89806	0.89676	0.20388	6.1443	6.0560
70.	0.92260	0.92204	0.15481	8.4091	8.3421
100	0.93512	0.93480	0.12975	10.232	10.176
200	0.95403	0.95391	0.09194	14.876	14.836
400	0.96746	0.96742	0.06508	21.464	21.436
700	0.97539	0.97537	0.04922	28.738	28.717
1000	0.97941	0.97940	0.04119	34.560	34.543
10000	0.99349	0.99348	0.01303	111.69	111.69

T A B L E I I

Distributions for $\varepsilon = 0$

	$u(x,\tau)$					
τ \ x	0.1	0.4	1.0	4.0	10.	40.
0.1	0.4330	0.3253	0.1837	0.0146		
0.4	0.4686	0.3646	0.2200	0.0168		
1.0	0.5270	0.4298	0.2834	0.0310	0.0002	
4.0	0.6820	0.6097	0.4801	0.1162	0.0034	
10.	0.7853	0.7349	0.6380	0.2684	0.0252	
40.	0.8992	0.8629	0.8106	0.5664	0.2176	
100	0.9295	0.9127	0.8792	0.7159	0.4314	0.0043

	$v(x,\tau)$					
τ \ x	0.1	0.4	1.0	4.0	10.	40.
0.1	0.0406	0.0302	0.0169	0.0008		
0.4	0.1472	0.1122	0.0651	0.0042		
1.0	0.3073	0.2427	0.1511	0.0133		
4.0	0.6320	0.5546	0.4214	0.0877	0.0021	
10.	0.7737	0.7207	0.6195	0.2460	0.0206	
40.	0.8878	0.8611	0.8082	0.5614	0.2120	
100.	0.9292	0.9122	0.8785	0.7146	0.4291	0.0042

TABLE III

Integrated Radiation Energy $\Psi_r(\tau)$ for $\varepsilon \neq 0$

τ \ ε	0.1	0.4	1.0	4.0	10.	40.	100
0.01	0.06822	0.01937	0.00809	0.00210	0.00085	0.00021	0.00008
0.02	0.12147	0.03682	0.01569	0.00413	0.00168	0.00042	0.00017
0.04	0.20320	0.06826	0.03002	0.00809	0.00332	0.00085	0.00034
0.07	0.28807	0.10929	0.04990	0.01382	0.00573	0.00147	0.00059
0.1	0.34587	0.14495	0.06832	0.01938	0.00809	0.00210	0.00085
0.2	0.44901	0.23817	0.12215	0.03688	0.01570	0.00413	0.00168
0.4	0.53860	0.36009	0.20747	0.06862	0.03008	0.00809	0.00332
0.7	0.63451	0.47682	0.30489	0.11093	0.05020	0.01385	0.00573
1.0	0.72438	0.56563	0.38332	0.14906	0.06910	0.01943	0.00810
2.0	1.0008	0.81135	0.59159	0.25924	0.12654	0.03721	0.01576
4.0	1.4757	1.2260	0.92854	0.44315	0.22736	0.07030	0.03038
7.0	2.0649	1.7417	1.3480	0.67694	0.35986	0.11614	0.05116
10.	2.5638	2.1793	1.7058	0.88071	0.47837	0.15886	0.07096
20.	3.8839	3.3408	2.6616	1.4400	0.81408	0.28676	0.13213
40.	5.8117	5.0420	4.0710	2.2889	1.3429	0.50338	0.24056
70.	7.9696	6.9498	5.6580	3.2630	1.9664	0.77493	0.38264
100	9.7070	8.4873	6.9393	4.0572	2.4825	1.0089	0.50913
200	14.133	12.407	10.211	6.1007	3.8278	1.6436	0.86557
400	20.414	17.971	14.861	9.0225	5.7726	2.5968	1.4240
700	27.349	24.117	19.999	12.261	7.9403	3.6834	2.0797
1000	32.900	29.036	24.113	14.857	9.6825	4.5664	2.6213
10000	106.44	94.221	78.645	49.325	32.892	16.516	10.148

TABLE IV

Integrated Material Energy $\psi_m(\tau)$ for $\epsilon \neq 0$

τ \ ϵ	0.1	0.4	1.0	4.0	10.	40.	100
0.01	0.00036	0.00010	0.00004				
0.02	0.00131	0.00038	0.00016	0.00004	0.00001		
0.04	0.00454	0.00142	0.00061	0.00016	0.00006	0.00001	
0.07	0.01176	0.00402	0.00178	0.00048	0.00020	0.00005	0.00002
0.1	0.02083	0.00767	0.00348	0.00096	0.00040	0.00010	0.00004
0.2	0.05747	0.02550	0.01233	0.00357	0.00150	0.00039	0.00016
0.4	0.13771	0.07636	0.04058	0.01263	0.00543	0.00144	0.00059
0.7	0.25490	0.16676	0.09765	0.03301	0.01459	0.00395	0.00162
1.0	0.36560	0.25953	0.16232	0.05847	0.02642	0.00728	0.00301
2.0	0.69576	0.54559	0.38124	0.15728	0.07489	0.02156	0.00906
4.0	1.2349	1.0158	0.75866	0.35205	0.17770	0.05405	0.02320
7.0	1.8741	1.5746	1.2119	0.60092	0.31659	0.10106	0.04430
10.	2.4011	2.0365	1.5890	0.81401	0.43945	0.14476	0.06440
20.	3.7664	3.2372	2.5761	1.3893	0.78321	0.27467	0.12625
40.	5.7276	4.9677	4.0093	2.2513	1.3192	0.49337	0.23544
70.	7.9057	6.8933	5.6108	3.2340	1.9477	0.76657	0.37818
100	9.6534	8.4399	6.8998	4.0327	2.4665	1.0015	0.50510
200	14.095	12.373	10.183	6.0831	3.8162	1.6380	0.86236
400	20.387	17.948	14.841	9.0100	5.7643	2.5926	1.4215
700	27.329	24.099	19.984	12.251	7.9339	3.6802	2.0777
1000	32.883	29.021	24.101	14.849	9.6772	4.5637	2.6196
10000	106.44	94.217	78.641	49.322	32.891	16.515	10.147